The effect of gait and digital flexor muscle activation on limb compliance in the forelimb of the horse *Equus caballus*

M. Polly McGuigan* and Alan M. Wilson

Structure and Motion Laboratory, Veterinary Basic Sciences, The Royal Veterinary College, Hawkshead Lane, North Mymms, Hatfield, Hertfordshire AL9 7TA, UK

*Author for correspondence at present address: School of Biology, L. C. Miall Building, University of Leeds, Leeds LS2 9JT, UK
(e-mail: m.p.mcguigan@leeds.ac.uk)

Summary

A horse's legs are compressed during the stance phase, storing and then returning elastic strain energy in spring-like muscle-tendon units. The arrangement of the muscle-tendon units around the lever-like joints means that as the leg shortens the muscle-tendon units are stretched. The forelimb anatomy means that the leg can be conceptually divided into two springs: the proximal spring, from the scapula to the elbow, and the distal spring, from the elbow to the foot. In this paper we report the results of a series of experiments testing the hypothesis that there is minimal scope for muscle contraction in either spring to adjust limb compliance. Firstly, we demonstrate that the distal, passive leg spring changes length by 127 mm (range 106–128 mm) at gallop and the proximal spring by 12 mm (9–15 mm). Secondly, we demonstrate that there is a linear relationship between limb force and metacarpo–phalangeal (MCP) joint angle that is minimally influenced by digital flexor muscle activation *in vitro* or as a function of gait *in vivo*. Finally, we determined the relationship between MCP joint angle and vertical ground-reaction force at trot and then predicted the forelimb peak vertical ground-reaction force during a 12 m s^{-1} gallop on a treadmill. These were 12.79 N kg^{-1} body mass (BM) (range 12.07–13.73 N kg^{-1} BM) for the lead forelimb and 15.23 N kg^{-1} BM (13.51–17.10 N kg^{-1} BM) for the non-lead forelimb.

Key words: locomotion, gait, stiffness, tendon, horse, *Equus caballus*.

Introduction

Large cursorial mammals have lengthened distal limb bones and tendons. The muscles of the distal limb associated with weight bearing have short muscle fibres, a pennate structure and significant passive elastic properties (Alexander et al., 1979, 1982; Biewener, 1998a; Dimery et al., 1986). Tendinous tissue is elastic and returns about 93% of the energy stored in it (Ker, 1981), thus the long tendons and muscle aponeurosis are used to store and return elastic energy during the stance phase of locomotion (Alexander, 1988; Alexander and Bennet-Clarke, 1977). The short fibres reduce the energetic cost of force generation. These adaptations result in a substantial reduction in the energetic cost of locomotion (Minetti et al., 1999; Roberts et al., 1997; Biewener et al., 1998), with the limb acting as a pogo-stick-like, tuned-spring system (Blickhan, 1989; Cavagna et al., 1977; McMahon, 1985; McMahon and Cheng, 1990). The limbs of smaller animals (including humans) also appear mechanically as compression springs (Farley et al., 1991, 1993; McMahon and Greene, 1979), but much of the length change occurs in muscle. This is energetically expensive due to the greater cost of force generation in long fibres and the requirement for muscle work (force × length change).

There is, however, a disadvantage in having a forelimb with mainly passive properties. Humans can change limb compliance as a function of surface compliance and stride frequency (Farley and Gonzales, 1996; Farley et al., 1998; Ferris and Farley, 1997). In this situation the muscles either store energy in the tendon, for subsequent release in a catapult mechanism when the muscle-tendon unit/limb is unloaded, lengthen and shorten to emulate spring-like properties, or preload the tendon and hence stiffen the spring (due to the non-linear force–length properties of tendon). As the muscle fibres become short in proportion to the tendon length there is less scope for control in the system, since the limited shortening of the associated muscle will only stretch the tendon rather than causing movement at the insertion (Biewener and Roberts, 2000).

In the horse the ground reaction force acts approximately along the axis of the leg from the foot to close to the attachment of serratus ventralis (J. Watson and A. M. Wilson, unpublished data). The leg changes length along this axis by flexion of the limb joints and can be considered as two compression springs in series.

The distal spring

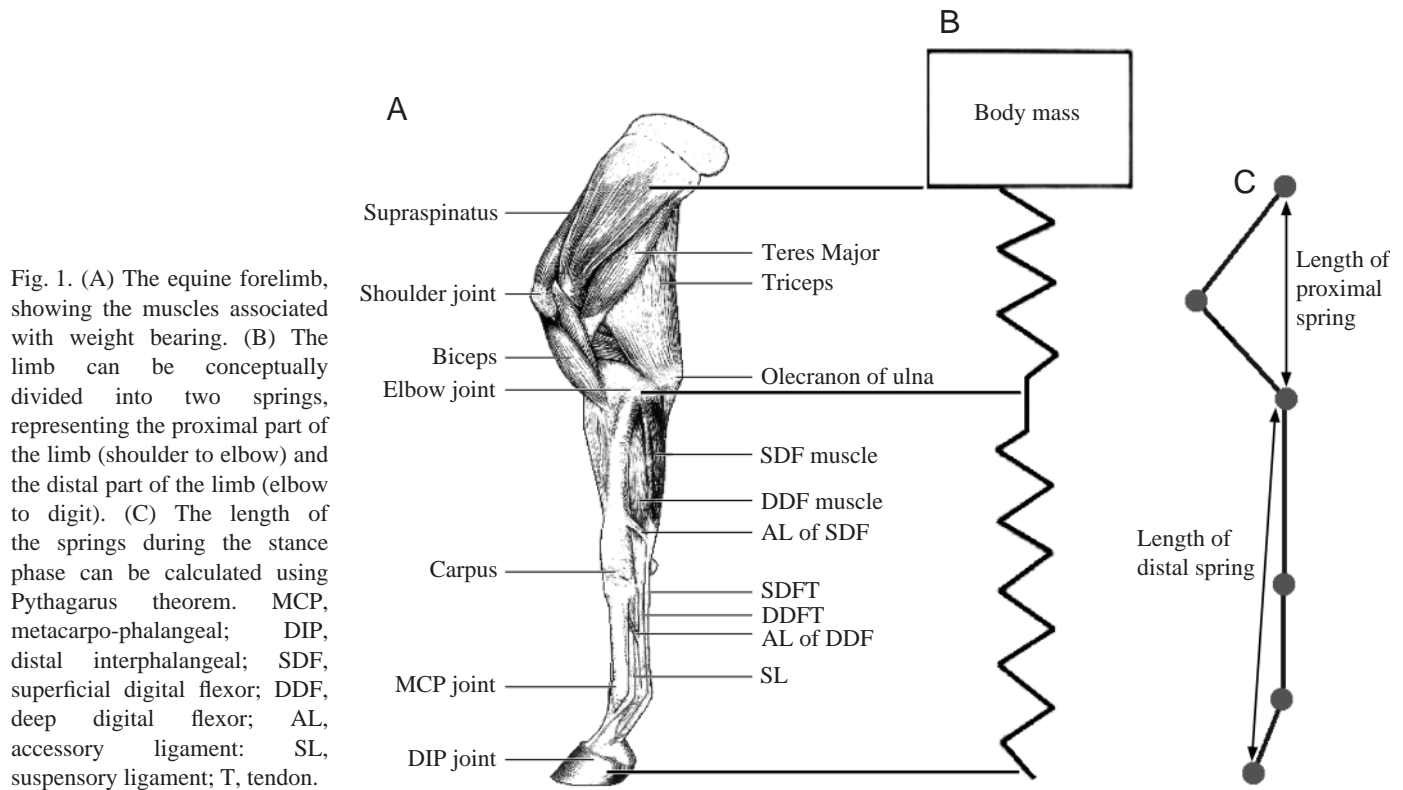The distal spring is the limb below the elbow joint, with

Fig. 1. (A) The equine forelimb, showing the muscles associated with weight bearing. (B) The limb can be conceptually divided into two springs, representing the proximal part of the limb (shoulder to elbow) and the distal part of the limb (elbow to digit). (C) The length of the springs during the stance phase can be calculated using Pythagarus theorem. MCP, metacarpo-phalangeal; DIP, distal interphalangeal; SDF, superficial digital flexor; DDF, deep digital flexor; AL, accessory ligament: SL, suspensory ligament; T, tendon.

length change occurring by extension of the metacarpo-phalangeal (MCP) and distal interphalangeal (DIP) joints.

Extension of the metacarpo-phalangeal joint during stance is resisted by three specialised muscle tendon units: the superficial and deep digital flexors (SDF, DDF) and the suspensory ligament (SL) (Dyce et al., 1987) (Fig. 1). These three structures are loaded to high strains and forces during locomotion (Biewener 1998a; Dimery et al., 1986; Meershoek et al., 2001; Stephens et al., 1989) and approx. 50% of racehorse injuries occur in these tendons (Williams et al., 2001). The SL, an evolutionary modification of the interosseus muscle, is completely fibrous, with in young animals, at most, only remnants of muscle fibres. The superficial digital flexor muscle is almost completely fibrous in the hind limb and in the forelimb has fibres of length 2–6 mm (Biewener, 1998b; Dimery et al., 1986; Hermanson and Cobb, 1992). The deep digital flexor muscle has three heads, humeral, radial and ulnar. The largest of these, the humeral head, has a mass of approximately 400 g and can be divided into three compartments by fibre length. The fibres are 7 ± 1 mm in the short-fibre compartment, 18 ± 1 mm in the intermediate-fibre compartment and 112 ± 13 mm in the long-fibre compartment (M. P. McGuigan and R. Hagan, unpublished data). The radial and ulnar heads are much smaller with fibres of approximately 17 mm (Hermanson and Cobb, 1992). The SDF and DDF muscles are force-protected by accessory ligaments (Dyce et al., 1987) that link the tendon distal to the muscle belly to the bone (Fig. 1). The force generation capacity of these muscles is about 5 kN (predicted from calculations of physiological cross-sectional area). The deep digital flexor muscle was shown to exert a force of about 3 kN in horses with chronic foot lameness (Wilson et al., 2001a). In those studies the effect of DDF muscle contraction was to stretch the associated tendon, since no change in foot position was observed. In a previous study we have, however, shown that, *in vitro*, the digital flexor muscles are only capable of a length change of a few millimetres (Wilson et al., 2001b).

The proximal spring

The proximal spring represents the limb between the scapula and the elbow, with length change along the ground reaction force (GRF) vector occurring *via* linked flexion of the shoulder and the elbow (Fig. 1).

Elbow flexion is resisted by the large triceps muscle and by the digital flexors (which have an extensor moment at the elbow), and shoulder flexion by the biceps and supra spinatus muscles and a number of other muscles (Dyce et al., 1987) (Fig. 1). The other muscles of the shoulder either have small moment arms on the joint and appear to act as stabilisers preventing out of sagittal plane movements, or are long-fibred and likely to be involved in limb movement rather than resisting gravitational and inertial forces.

The proximal limb spring is therefore both muscular and collagenous in nature (Fig. 1). The relative role of the two leg springs is of interest. One possible role is that the proximal spring acts in series with the mainly passive distal limb spring to tune the properties of the whole limb for locomotion under varying conditions. This mechanism could be simply *via* the
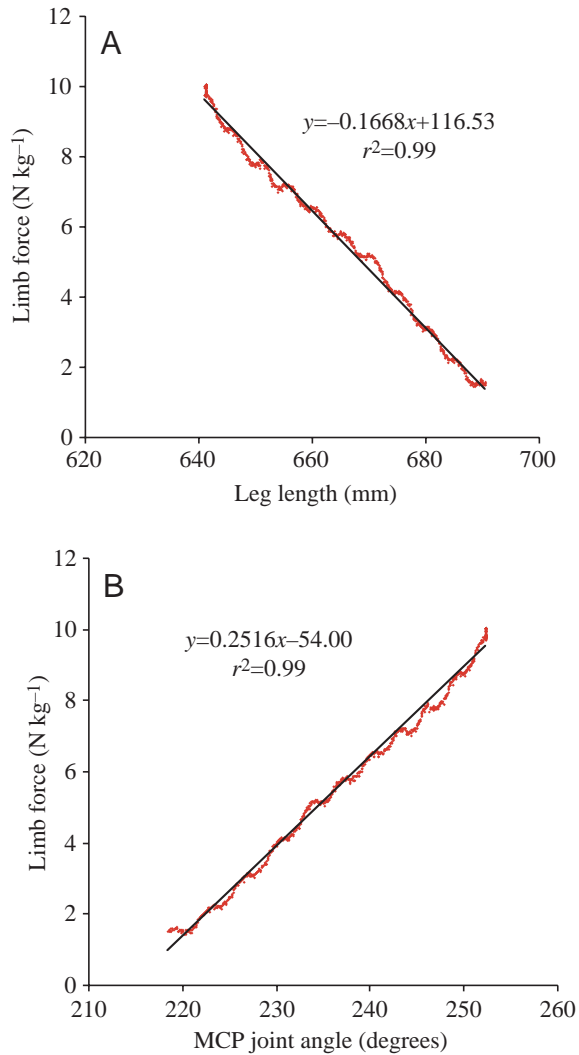
Fig. 2. (A) Leg length (centre of rotation of the elbow joint to the hoof) and (B) metacarpo-phalangeal (MCP) joint angle–limb force relationship for an equine distal limb during *in vitro* loading. The solid lines are linear regression lines: (A) $y=-0.2089x+132$, $r^2=0.996$ and (B) $y=0.3821x+78.0$, $r^2=0.994$.

mechanical effect of two springs in series and changing the stiffness of the proximal spring *via* muscle contraction. In addition, changing the elbow angle by muscle contraction will change the zero length of the digital flexor muscles. Due to alterations in load distribution between the long and compliant muscle belly and the short and stiff accessory ligament, this would also have a tuning effect on leg stiffness. Alternatively, the proximal spring muscles may act to drive the distal spring, either by a power flow across the elbow or by shortening in late stance as the leg unloads.

Muscle shortening during stance is, however, energetically expensive, due to the high forces in the muscles that resist the ground reaction force and the relatively long muscle fibres that are required. Optimisation of the musculoskeletal system for economical locomotion would therefore suggest that length change should occur in the distal, passive, spring and that the

muscles of the proximal spring would remain isometric during stance. Length change in the proximal spring would therefore be limited to elastic deformation of the elastic elements of the muscle tendon unit. Biceps, in addition to its antigravity role, functions as the spring in a catapult mechanism to protract the limb (Wilson et al., 2003).

The attachment to the trunk could be considered as a third spring, which is muscular in nature, but that will not be discussed further here.

The present work reports the results of a series of experiments where the compliance of the limb under varying locomotor conditions was examined, with the aim of determining if a horse can alter limb compliance.

This study tested the following two hypotheses: (1) the majority of the length change in the equine forelimb occurs below the elbow joint in the collagenous distal limb; and (2) the relationship between MCP joint angle and limb force is similar for limbs loaded *in vitro* and *in vivo*, and is not altered by contraction of the digital flexor muscles *in vitro* or by changing gait *in vivo*.

Four experiments were undertaken. (1) Length changes in the proximal and distal forelimb during stance phase of locomotion were measured at a range of speeds and gaits on the treadmill. (2) The MCP joint angle–limb force relationship *in vitro*, and how it is altered by contraction of the digital flexor muscles, and (3) *in vivo*, and how it is altered by gait, were examined. (4) The peak vertical GRF at gallop was estimated from the MCP joint angle–limb force relationship.

Materials and methods

(1) Proximal and distal length change in the forelimb

Flat, circular, retro-reflective markers (Scotchlite 8850, 3M, Manchester, England) 20 mm in diameter were placed at the following skeletal landmarks on the left forelimbs of four clinically normal thoroughbred horses *Equus caballus* L.: the proximal end of the spine of the scapula, the caudal part of the greater tubercle of the humerus (centre of rotation of the shoulder joint), the lateral epicondyle of the humerus (centre of rotation of the elbow joint), the lateral styloid process of the radius, the proximal end of metacarpal IV, the proximal attachment of the lateral collateral ligament of the MCP joint to the distal metacarpal III (centre of rotation of the MCP joint), and the lateral hoof wall, approximately over the centre of rotation of the DIP joint.

The horses were then exercised on a high-speed treadmill. The positions of the markers were recorded using a 3-D video motion analysis [ProReflex 2.5, Qualisys AB, Göteborgsvägen 74, SE-433 63, Sävedalen, Sweden (www.Qualisys.com)] system positioned approximately 2 m to the left of the treadmill.

The horses were fully habituated to the treadmill (Sato, Upsalla, Sweden) (Buchner et al., 1994) and were exercised on it regularly. During the test they wore neoprene brushing boots and over-reach boots to avoid interference injuries while galloping at high speed.

After a warm up period of 5 min walk and 5 min trot, data were recorded at 120 Hz during the last 10 s of a 1 min period of trot (3.5 m s^{-1}), canter (6 m s^{-1} and 8 m s^{-1}) and gallop (12 m s^{-1}).

The cranio-caudal and vertical position of the markers on the proximal spine of the scapula, the centre of rotation of the elbow joint and the hoof wall were determined at the beginning of the stance phase and at mid-stance. The beginning of the stance phase was taken to be the time point at which the vertical coordinate of the foot marker became constant at the end of the protraction phase, and mid-stance was defined as the time point at which the metacarpal bone was vertical (i.e. the marker at the proximal end of metacarpal IV was above the marker at the MCP joint). From these coordinates the lengths of the proximal and distal portions of the limb were calculated using Pythagarus' theorem in a spreadsheet program (Excel 97, Microsoft, USA).

The proximal spring length was defined as the distance between the proximal spine of the scapula and the elbow joint, and the distal spring length as the distance between the elbow joint and the hoof. The length change during stance was defined as the difference between the values at the beginning of stance and mid-stance. These were expressed as absolute length changes and ratios of proximal:distal length changes.

(2) In vitro MCP joint angle–limb force relationship

Tissue was collected from horses of varying size, breed and age, euthanased at the Royal Veterinary College and an equine abattoir for reasons other than orthopaedic problems. Immediately *post mortem* one forelimb was removed and prepared for loading in a hydraulic testing machine.

Mounting the limb

Limbs were sectioned with the humero–radial (elbow) joint held at an angle similar to that seen at mid-stance (230–235°). The limbs were cut with a saw at right angles to the long axis of the distal limb just proximal to the humeral epicondyles, leaving the olecranon intact. A 13 mm diameter hole was drilled vertically down from the marrow cavity of the distal humerus through the elbow joint articulation and into the radius. The limbs were mounted in the hydraulic loading jig (Clarke machinery 020410000, www.machinemart.co.uk) by means of a 130 mm pin, which was positioned vertically down through the elbow joint and attached to a hydraulic ram. The pin was placed down the drilled hole so that the sectioned humerus rested on the face of the ram. The ram face provided a 50 mm diameter flat loading surface. This pin locked the elbow joint to prevent any change in joint angle during loading but was not rigidly fixed to the ram, to allow cranio–caudal movement of the intermediate segments of the limb (Wilson et al., 2001b). The hoof of the limb was positioned on a base plate. Compression of the ram resulted in compression of the limb and extension of the carpus, MCP and DIP joints.

In order to stimulate the digital flexor muscles and assess the effect of stimulation, the limbs were prepared as follows: flexor carpi radialis, flexor carpi ulnaris and extensor carpi ulnaris

were removed. The tendons on the dorsal aspect of the limb of the digital extensor muscles and extensor carpi radialis were sectioned proximal to the carpus (this was done to prevent voltage leakage from the stimulator causing activation and force generation of these muscles).

The digital flexor muscles were stimulated using an electrical stimulator under the control of a signal generator, and clean 128-strand copper wires placed proximally and distally in the muscles. The stimulator supplied a 60 V signal at 50 Hz with a pulse duration of 0.06 ms. Once the electrodes were in place the muscles were wrapped in plastic film to prevent evaporative cooling. The experiments were completed by 1 h *post mortem*.

Measurements

The hoof of the limb was positioned on a foot-plate. A shear beam force transducer (Transducer World, Aylesbury, Buckinghamshire) placed under the foot-plate recorded axial limb force, logged at 100 Hz *via* software written in LabView [National Instruments, Newbury, Berkshire RG14 5SJ, UK (www.natinst.com)]. The amplified output from the force transducer was displayed on a voltmeter so that limb force could be controlled during the loading cycles. The output from the signal generator was also logged *via* LabView.

MCP joint angle and limb length were calculated from kinematic data collected at 100 Hz using a 2-D video motion analysis system (ProReflex 2.5). Flat, circular retro-reflective markers 10 mm in diameter were placed at the following anatomical landmarks to facilitate calculation of MCP joint angle and the length of the limb during the compressive loading: the origin of the digital flexor muscles, the proximal end of metacarpal II, the proximal attachment of the lateral collateral ligament of the MCP joint to the distal metacarpal III and the lateral hoof wall approximately over the centre of rotation of the DIP joint.

Two flat markers were placed on the frame of the loading jig, 300 mm apart, for length-calibration purposes.

Simultaneous limb force, electrical stimulation and kinematic data were recorded for a preiod of 15 s while the limb was ramp loaded to approximately 1.25× body mass, with and without muscle stimulation. Four unstimulated and two stimulated (both DDF and SDF muscles) loading cycles were recorded. Recordings were made from six limbs in the unstimulated and stimulated states and a further three limbs in the unstimulated state only.

MCP joint angle (around palmar aspect) and limb length were calculated using trigonometry in a spreadsheet program and plotted against limb force for the loading phase of the cycle. Linear regression lines were calculated for each trial of each limb. A mean plot for unstimulated loading of each limb was generated and compared to the first and second stimulated loadings. Paired *t*-tests were used to compare the force required to produce an MCP joint angle of 220° during the unstimulated loadings with the force required to produce the same joint angle during the first and second stimulated loadings.

(3) In vivo MCP joint angle–limb force relationship

Horses and riders

Seven thoroughbred-cross riding horses of mixed size and age were used. They were all assessed as having a 'normal' gait and being free from any signs of lameness on veterinary examination. All the horses were accustomed to being ridden in the indoor arena where the data were recorded. The data were recorded during ridden locomotion and all the horses were ridden by riders with whom they were familiar. Three different riders were used. The mass of the horses was 548–667 kg and that of the riders 60–70 kg.

Experimental setup

A forceplate (Kistler 9827BA, Kistler Instruments Ltd. Alresford House, Mill Lane, Alton, Hampshire GU34 2QJ) was buried half way along the long side of an indoor riding arena (60 m×20 m). The mounting frame for the forceplate was set in 1 m^3 of concrete and the top of the plate was level with the sub-base of the riding surface. The forceplate was topped with an aluminium plate covered in a coarse surface conveyer belt matting and the riding surface, 200 mm of sand and polyvinyl chloride (PVC), was laid on top. The forceplate signal was amplified by integral eight-channel charge amplifiers, filtered through a low-pass filter (6 db/octave from 50 Hz) and logged *via* a 12-bit AD converter at 480 samples s^{-1} into a personal computer using software written in LabView (National Instruments).

The motion analysis system used above was placed to the left-hand side of the forceplate and calibrated relative to the forceplate to determine the position of the left forefoot relative to the plate and the left forelimb MCP joint angle during stance. Kinematic data were recorded at 240 Hz. The accuracy of the 3-D motion analysis system within a calibrated volume of 3 m×1 m×2 m was determined using a pre-calibrated grid and found to be within ±2 mm for absolute position measurements and less than ±0.1 mm for relative (i.e. length) measurements. Data logging for both systems was triggered using a light gate.

Recording protocol

Synchronised kinetic and kinematic data were recorded as each horse was ridden over the forceplate at walk, trot and canter (leading with left and right limbs), and jumped onto the forceplate until at least six left forestrikes had been recorded. (The speed within each gait was that chosen by the individual horses.) Data were rejected if the horse was not judged to be moving freely and consistently in a straight line, or the foot was not completely on the plate. The jump was a 750 mm high fence, situated 1.5–2 m in front of the forceplate, which was jumped from a steady canter. The horses were jumped onto the forceplate in an attempt to perturb the spring mass system. Jumping perturbs the system as stance time and the angle of the limb at impact are altered independently of speed.

Data analysis

Stance was defined as the period during which the vertical ground reaction force was greater than 50 N (Clayton et al., 1999). During analysis, data were rejected if the point of application of the GRF on the forceplate was within 100 mm of the edge of the plate. GRF data were normalised for the mass of the horse and rider and interpolated to 100 points, evenly spaced throughout the stance period, to allow the averaging of several strides (Merkens et al., 1985; Wilson et al., 1998). A plot of vertical GRF (mean ± S.D.) was produced for each horse at each gait.

MCP joint angle was defined as the angle around the palmar aspect of the limb and calculated from the cranio-caudal and vertical positions of the three limb markers by simple trigonometry. Foot-on and foot-off were determined from the simultaneous forceplate data and the MCP joint angle data were was normalised for stance time; plots of MCP joint angle (mean ± S.D.) were produced for each horse at each gait.

The corresponding mean vertical GRF and MCP joint angle during stance were plotted against one another to show the relationship between limb force and MCP joint angle within the stance phase for each gait/horse combination. Two linear regression lines were calculated for each of these plots: one for the loading phase of stance (impact to peak vertical force) and one for the unloading phase (peak vertical force to foot-off). The distribution of the data used to calculate the regression lines was skewed towards the upper end of the range due to the mid-stance plateau of the GRF curve (Fig. 6), hence the regression lines were weighted in that direction. The stiffness of the limb during the loading and unloading phases of stance was taken as the gradient of the respective regression line. This is not classical stiffness, since it is the relationship between a linear force and an angle change; it is, however, a useful measure for this study. The limb force associated with an MCP joint angle of 230° was calculated from the regression line of the loading phase of the MCP joint angle–limb force relationship for each horse at each gait. These values were compared using a single-factor analysis of variance (ANOVA) to determine if gait had a consistent effect on the relationship. In all statistics, $P \leq 0.05$ was considered to be a significant difference.

Peak values of vertical GRF and MCP joint angle, and the time of the peak for each horse at each gait, were calculated. The peak vertical GRF and MCP values for each horse at each gait were plotted against each other to assess the relationship between the peak values across gaits and horses. A linear regression line was calculated for each set of data points and separately for all the points together. Whilst statistically suspect, this served to illustrate whether the relationship between peak vertical GRF and peak MCP joint angle varied between gait and horses.

(4) Estimation of peak vertical ground reaction force at gallop

Five fit thoroughbred horses *Equus caballus*, free from any sign of lameness, were used in this part of the study (mass 524–678 kg).

Table 1. *Mean (range) length changes in the left forelimb of four horses during the stance phase of trot (3.5 m s⁻¹), right lead canter (6 m s⁻¹ and 8 m s⁻¹) and right lead gallop (12 m s⁻¹)*

	Speed (m s⁻¹)			
	3.5	6	8	12
Proximal length change (mm)	12 (6–14)	6 (4–9)	11 (3–16)	12 (9–15)
Distal length change (mm)	80 (67–86)	86 (68–96)	96 (80–109)	127 (106–128)
Ratio of mean length change Distal:Proximal	7.9	15.2	12.7	10.0

Proximal length change is that which occurs between the proximal scapula and the elbow joint; distal length change is that which occurs between the elbow and the hoof ($N=4$).

Determination of limb force–MCP joint angle relationship at trot

The forceplate was placed midway along a 25 m covered, concrete runway. The runway and the forceplate were covered in 6 mm thick commercial conveyer belt matting. The experimental setup was otherwise identical to that described above in (3).

Retro-reflective markers were placed at the skeletal landmarks described above to determine MCP joint angle, and a fourth marker was placed on the thorax of the horse to determine speed during forceplate assessment. The horses were trotted, in hand, at a speed comfortable for the horse, along the runway until six left forelimb forceplate strikes had been recorded.

Data were analysed as described above and plots of vertical GRF and MCP joint angle (mean ± S.D.) during stance generated. Peak vertical GRF and MCP joint angles were calculated, and the linear regression line for the loading and unloading phase of the limb force–MCP joint angle relationship calculated.

MCP joint angle at gallop

The same five horses were exercised on the treadmill (a 8 mm thick conveyer belt mat on a steel base plate with similar surface characteristics to the overground runway) to determine the peak MCP joint angle at gallop. The horses were habituated to the treadmill with three training sessions (Buchner et al., 1994; T. Richmond and A. W. Wilson, unpublished data). The experimental setup was similar to that described in (1). The retro-reflective markers remained *in situ* from the horses' overground assessment.

After a 'warm up' period, kinematic data were recorded for 10 s at the end of a 60 s exercise period on the flat at gallop (12 m s⁻¹). During the gallop test it was recorded whether the left forelimb was the lead or non-lead leg. We attempted to record trot data to verify that MCP joint angle was similar at the same speed of trot on the treadmill and overground, but unfortunately, a consistent trot could not be established on the treadmill at the over-ground speed. Maximum MCP joint angle during the stance phase was calculated for each stride and averaged for lead and non-lead limbs at gallop.

Peak vertical ground reaction force at gallop

The equations of the linear regression lines calculated for the limb force–MCP joint angle relationship at trot overground were used to predict the value of vertical GRF associated with the peak MCP joint angles observed at gallop.

Results
(1) Proximal and distal length changes in the forelimb

The total length change (proximal + distal length changes) of the limb during the stance phase was similar at trot and slow canter, and increased with speed of canter and gallop (Table 1). Between 87% and 91% (range) of the length change occurred in the distal portion of the limb between the elbow and the hoof. The length change at trot (3.5 m s⁻¹) ranged from 6 mm to 14 mm in the proximal segment (scapula to elbow) and from 67 mm to 86 mm in the distal segment (elbow to hoof). At gallop (12 m s⁻¹) the length change was 9–15 mm in the proximal segment and 106–128 mm in the distal segment. The mean ratio of proximal to distal spring length change and hence stiffness (since both experience the same force) was 7.9 at trot and 10.0 at gallop.

(2) In vitro MCP joint angle–limb force relationship

There was an excellent linear relationship ($r^2>0.99$) between the length of the limb and the force applied and MCP joint angle and the force applied to the limb throughout the loading cycle for all the loading trials (Fig. 2A,B). Fig. 3 shows the linear regression lines for the MCP joint angle–limb force relationship for the nine limbs in the unstimulated state. The r^2 values for these lines were 0.989–0.996 and the mean slope of the line was 0.34±0.02 N kg⁻¹ BM deg.⁻¹, range 0.32–0.37 N kg⁻¹ BM deg.⁻¹ in the different limbs. Six of the limbs were loaded with stimulation of the digital flexor muscles. There was minimal difference in the force required to produce a joint angle of 220° with (6.50±0.48 N kg⁻¹ BM) and without (6.45±0.41 N kg⁻¹ BM) contraction of the digital flexor muscles (values calculated from the regression lines) (Fig. 4).

(3) In vivo MCP joint angle–limb force relationship

Foot contact on the forceplate was difficult to confirm during data logging due to the riding surface covering the plate; some data were therefore rejected at the analysis stage because the point of application of the GRF on the forceplate was within 100 mm of the edge of the plate, indicating that the entire GRF had not been transmitted through the
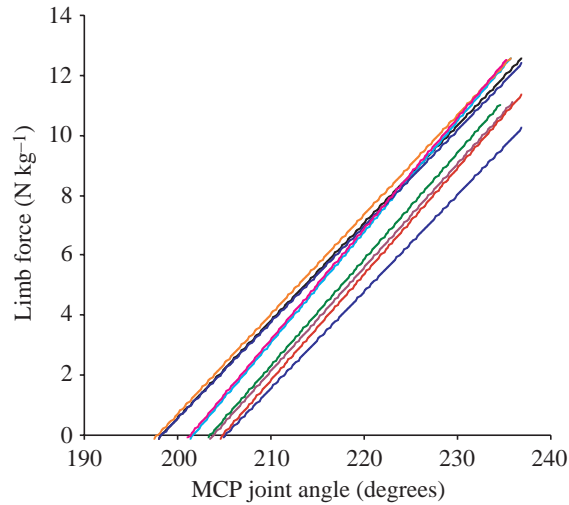
Fig. 3. Linear regression lines of the metacarpo-phalangeal (MCP) joint angle–limb force relationship for nine distal limbs during *in vitro* loading. r^2 values for these relationships were 0.983–0.996.
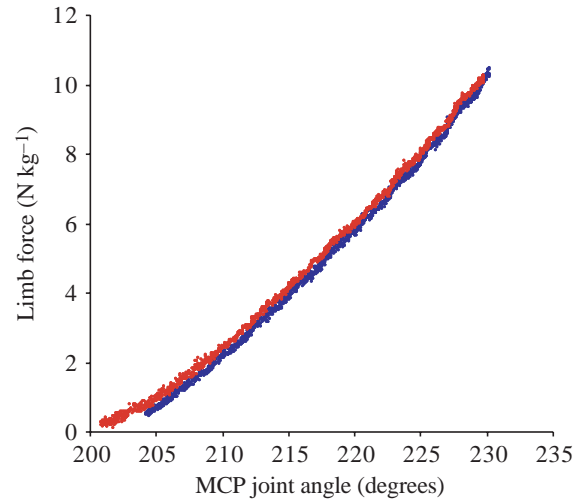

Fig. 4. Metacarpo-phalangeal (MCP) joint angle–limb force relationship for an equine distal limb during unstimulated (blue) and stimulated (red) *in vitro* loading.

forceplate. If three or fewer runs were left after this rejection, we did not calculate mean vertical GRF and MCP joint angle graphs for that horse/gait. Data are therefore not reported for lead canter in horses 5, 6 and 7 and non-lead canter for horse 4.

Representative graphs (4 runs) of vertical GRF and MCP joint angle (means ± 1 S.D.) during the stance phases of walk, trot, lead canter, non-lead canter and jump landing are shown in Fig. 5A–E. The S.D. values of both variables were small, demonstrating the very repeatable nature of the gaits. The two sets of plots have the same shape during stance and are similar to those reported previously for ridden and riderless locomotion. Peak MCP joint angle occurred 10–20 ms after the vertical GRF peaked. Peak MCP joint angles and mass-specific vertical GRFs increased from walk (216±5° and 6.16±0.53 N kg^{-1} BM, respectively) to trot (232±4° and 10.73±1.22 N kg^{-1} BM, respectively) and trot to non-lead canter (238±7° and 11.95±0.66 N kg^{-1} BM, respectively). The non-lead forelimb at canter experienced a greater peak MCP joint angle and peak vertical GRF than the lead forelimb (228±2° and 9.74±1.40 N kg^{-1} BM, respectively) (Table 2). The peak values for jump landing were less predictable

(234±6° and 10.60±1.27 N kg^{-1} BM, respectively): in five horses the peak values were similar or lower than those seen at trot, whereas in two horses they were greater than the peak values for the non-lead limb at canter.

The relationship between MCP joint angle and vertical GRF is shown for one horse at trot in Fig. 6. r^2 values for the linear regression lines calculated for the loading and unloading phases of the relationship were all greater than 0.95, showing that there is a very strong positive correlation between MCP joint angle and vertical GRF at all gaits. The mean stiffness of the MCP joint during loading in trot locomotion was 0.29±0.03 N kg^{-1} deg.$^{-1}$, range 0.25–0.35 N kg^{-1} deg.$^{-1}$ for the seven horses. The mean functional stiffness of the MCP joint during unloading in trot locomotion was 0.27+0.03 N kg^{-1} deg.$^{-1}$, range 0.24–0.33 N kg^{-1} deg.$^{-1}$. The relationship, and hence distal limb stiffness, was very similar at the different gaits (walk, trot, non-lead canter, lead canter and jump landing) (Fig. 7). The vertical GRFs required to produce an MCP joint angle of 230° were calculated using the linear regression lines for the loading and unloading phases of stance and are shown in Table 2. A single-factor ANOVA showed that there was no gait effect on the calculated vertical

Table 2. *Peak MCP joint angle, vertical GRF and the vertical GRF associated with an MCP joint angle of 230° (calculated from linear regression lines of the loading phase of the MCP joint angle–vertical GRF relationship for each horse/gait) during the stance phase of walk, trot, lead canter, non-lead canter and jump landing*

	Walk	Trot	Lead canter	Non-lead canter	Jump landing
Peak MCP joint angle (degrees)	216±5	232±4	228±2	238±7	234±6
Peak vertical GRF (N kg^{-1})	6.16±0.53	10.73±1.22	9.74±1.40	11.96±0.66	10.60±1.27
Vertical GRF at MCP joint angle of 230° (loading) (N kg^{-1})	9.25±1.13	9.99±1.23	10.49±1.22	9.40±1.23	9.80±1.88
Vertical GRF at MCP joint angle of 230° (unloading) (N kg^{-1})	9.66±1.80	9.39±1.23	9.67±1.16	8.83±1.34	8.74±1.00

Values are means ± S.D. (*N*=4–7).
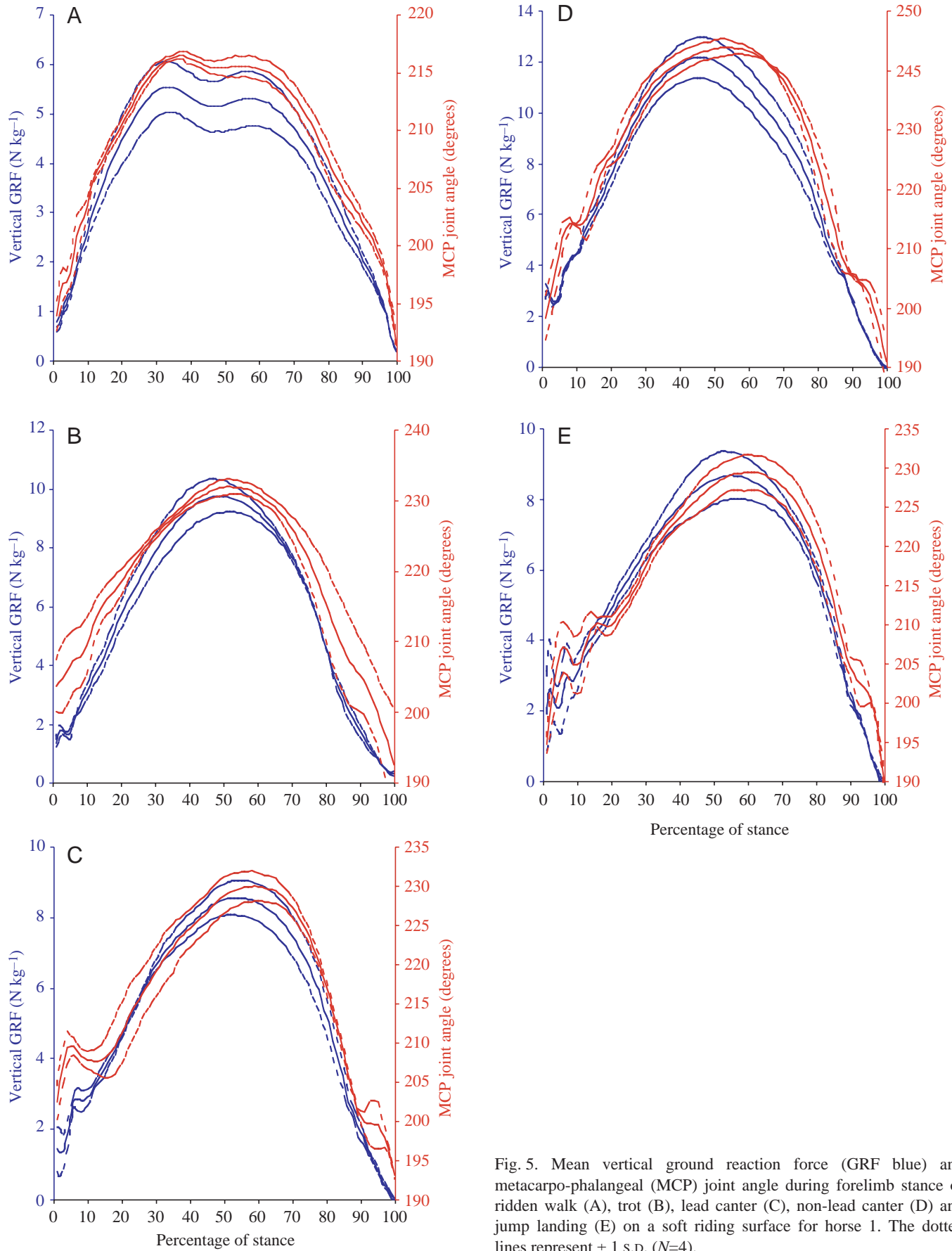MCP, metacarpo-phalangeal; GRF, vertical ground reaction force.

Fig. 5. Mean vertical ground reaction force (GRF blue) and metacarpo-phalangeal (MCP) joint angle during forelimb stance of ridden walk (A), trot (B), lead canter (C), non-lead canter (D) and jump landing (E) on a soft riding surface for horse 1. The dotted lines represent ± 1 S.D. (N=4).
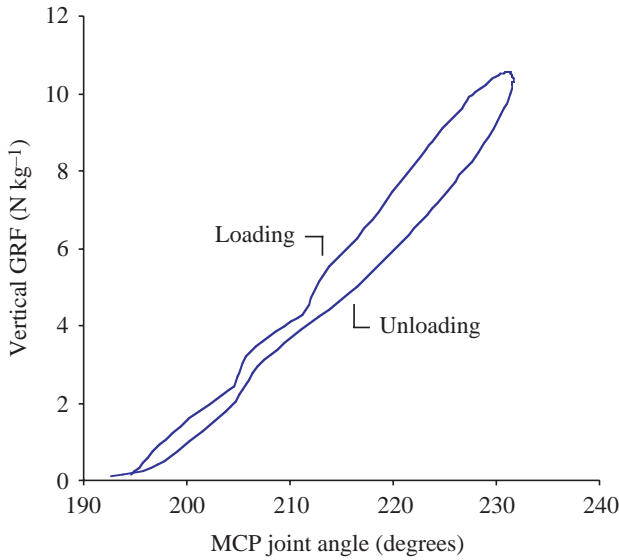
Fig. 6. A typical plot of the relationship between metacarpo-phalangeal (MCP) joint angle and vertical ground reaction force (GRF) during the stance phase of trot for one horse.

GRF for a joint angle of 230° at different gaits. The values for jump landing were, however, more variable than the values for other gaits. There was ±4–11% range around the mean in the calculated values including the values for jump landing, and ±2–7% range around the mean excluding the values for jump landing.

The values of vertical GRF for a MCP joint angle of 230° were lower for the unloading phase than the loading phase of the relationship at trot ($P<0.01$), lead canter ($P=0.02$), non-lead canter ($P=0.03$) and jump landing ($P=0.03$) (Table 2).

Fig. 8 shows peak MCP joint angle plotted against peak

Fig. 8. Peak metacarpo-phalangeal (MCP) joint angle *versus* peak vertical ground reaction force (GRF) for each gait of each horse. The different symbols represent the different horses. Linear regression lines are shown for each horse. The black broken line represents the relationship between MCP joint angle and vertical GRF for the population of horses; $y=0.2113x-38.68$, $r^2=0.70$.

vertical GRF for each horse in each different gait. Each horse is represented by a different symbol on the graph. The regression lines for each horse show that there is a linear relationship between the two parameters across different gaits ($r^2=0.90$–0.99). A regression for the group of horses shows that a similar relationship exists across a group of horses ($r^2=0.70$, $P<0.001$).
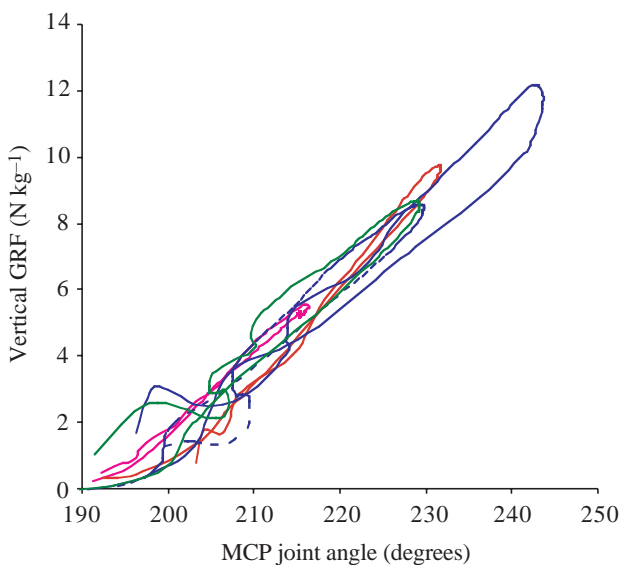

Fig. 7. The relationship between metacarpo-phalangeal (MCP) joint angle and vertical ground reaction force (GRF) during the stance phase of walk (pink), trot (red), lead canter (blue dashed), non-lead canter (blue) and jump landing (green) for horse 1.
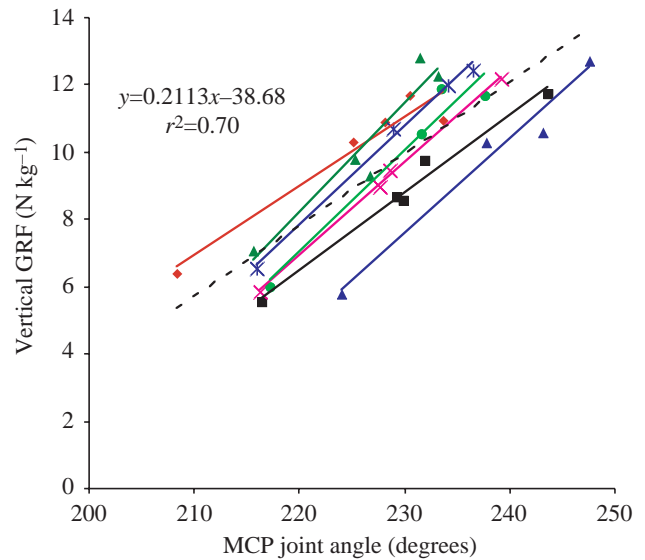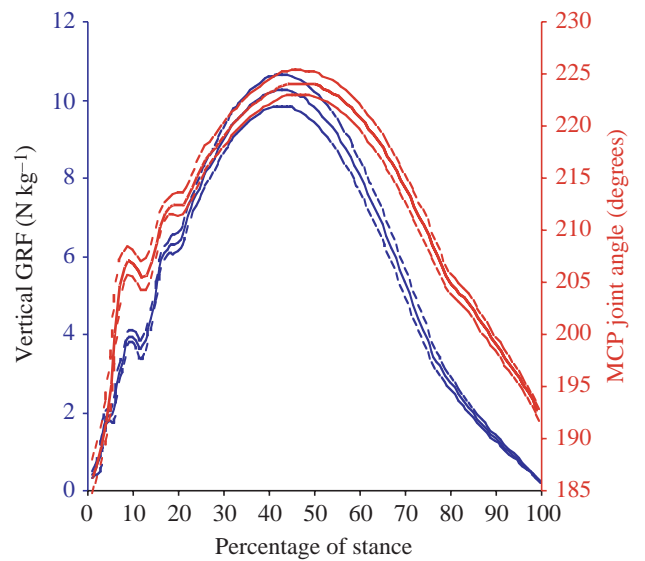

Fig. 9. Mean vertical ground reaction force (GRF; blue) and metacarpo-phalangeal (MCP) joint angle (red) during forelimb stance of in-hand trot on a hard surface for one horse. The dotted lines represent ± 1 s.D. ($N=4$).

(4) Estimation of peak vertical ground reaction force at gallop

Mean vertical GRF and MCP joint angles during the stance phase of trot on a hard surface for one of the horses are shown in Fig. 9. Comparison with data generated on a soft surface (Fig. 5B) demonstrates that the limb loaded more rapidly on the hard surface but the limb unloaded at a similar rate on both surfaces. As a result of this, peak vertical GRF and peak MCP joint angle occurred earlier on the hard surface. The loading portion of both the vertical GRF and MCP joint angle showed much more high-frequency oscillation on the hard surface (Fig. 9) than on the soft surface (Fig. 5B).

The equations of the linear regression lines calculated for the loading phase of the overground trot data for each horse were used to estimate the vertical GRF required to achieve the peak MCP joint angles recorded at gallop on the treadmill. The left forelimb was the lead forelimb in two horses and the non-lead forelimb in two horses. Data were collected from one horse whilst galloping on both leads. Peak MCP joint angle was 237.6° (range 234°–240.4°) for the lead forelimb and 245.3° (range 241.8°–248.1°) for the non-lead forelimb. Estimated peak vertical GRF at gallop was 12.79 N kg^{-1} BM (range 12.07–13.73 N kg^{-1} BM) for the lead forelimb (N=3) and 15.23 N kg^{-1} BM (13.51–17.10 N kg^{-1} BM) for the non-lead forelimb (N=3).

Discussion

The proximal spring was approximately ten times as stiff as the distal spring. Although there is a fibrous component of biceps the majority of the proximal spring is made up of muscle. It may be speculated that the muscular component of the proximal spring is used to tune the limb for locomotion by changing limb stiffness. The formula for the combined stiffness of two springs of stiffness, k_p and k_d (proximal and distal, respectively), in series is $k_p \times k_d / k_p + k_d$. The stiffness of the distal spring (calculated from the *in vitro* relationship between limb length and limb force; Fig. 2A) was approximately 60 kN m^{-1}. The length change in the distal spring is ten times greater than the length change in the proximal spring; both springs experience the same GRF, hence the proximal spring is ten times stiffer than the distal – an approximate value of 600 kN m^{-1}. This results in an overall leg stiffness of 55 kN m^{-1}. Reducing the stiffness of the proximal spring by 50% to 300 kN m^{-1} would decrease whole leg stiffness to 50 kN m^{-1}, and increasing the stiffness of the proximal spring by 100% to 1200 kN m^{-1} would increase whole leg stiffness to 57 kN m^{-1}. These are both relative small changes for a very substantial change in proximal limb stiffness and suggest that muscular action in the proximal spring would have minimal tuning effect on limb stiffness. By comparison, changing surface stiffness from a figure representative of tarmac to one representative of turf (k=500 kN m^{-1}), which permits a 50 mm deformation at mid-stance, changes limb stiffness from 55 kN m^{-1} to 50 kN m^{-1} and changes limb resonant frequency by 7% (Wilson et al.,

2001b). Doubling proximal spring stiffness (to 1200 kN m^{-1}) only returns this to 51 kN m^{-1}. It is therefore unlikely that the proximal spring has sufficient capacity to tune the leg stiffness as a function of surface. The role of the proximal spring may be to achieve a small tuning effect and/or to drive the distal limb spring (i.e. to compensate for hysteresis and surface energy losses). In addition, biceps needs to be stiff for its role in limb protraction (Wilson et al., 2003), which would limit its function as a stance phase energy store. There may, however, be some additional tuning of limb stiffness from the muscles that attach the limb to the trunk (particularly serratus ventralis).

The determination of length change in the proximal portion of the limb is less accurate than the distal limb, due to the effect of skin displacement. The movement of the skin relative to the underlying skeletal landmarks is much greater in the proximal limb than the distal limb (van Weeren et al., 1990). During the stance phase there is 5–10 mm of skin displacement relative to the proximal spine of the scapula both along the axis of the bone and perpendicular to it, but there is minimal skin displacement at the elbow joint (van Weeren et al., 1990). The skin displacement perpendicular to the scapula would be expected to have some influence on the results reported but not sufficient to alter the conclusions of the paper.

The relationship between MCP joint angle and limb force was similar in different horses and gaits. This is similar to the results of Farley et al. (1993) who showed that limb stiffness does not increase with increasing speed across a range of species. The stiffness of the limb determines the natural frequency of the spring mass locomotion model, hence, similar limb stiffness would be predicted as similar sized horses have similar stride frequencies (Leach and Cymbaluk, 1986). Superficial digital flexor tendon stiffness varies by a factor of two between different thoroughbred horses (Wilson, 1991) so the lever arms of the tendons or the stiffness of other structures must compensate for this. Stance time drops with speed, but the time required to protract the limb is relatively independent of gait and speed in the horse (Wilson et al., 2000). Whilst the sweep of the limb during stance rises somewhat (Farley et al., 1993), this increase is insufficient to prevent the drop in stance time. The proportion of time spent in stance (duty factor) therefore drops with speed (Biewener 1983; Pratt and O'Connor, 1978). Since average limb force over time must equal body weight this results in an increase in peak vertical GRF, a greater MCP joint angle and, hence, a greater compression of the distal limb spring. The only joint with significant capacity to create length change in the distal limb is the MCP joint. Bone and tendon strain also rise with speed, presumably due to the increased peak limb force and increased extension of the MCP joint (McLaughlin et al., 1996; Pratt and O'Connor, 1978; Rubin and Lanyon, 1987; Stephens et al., 1989).

The similarity of limb stiffness in different horses also provides an explanation for the apparent quiescence of energy-storing tendons in response to changes in mechanical environment (Wilson, 1991; Birch et al., 1999). If a tendon were to hypertrophy it would be stiffer, which would diminish

its ability to store and return energy at an appropriate rate during the gait cycle and alter the frequency of the spring mass system.

The slope of the MCP joint angle–limb force relationship was 10% higher *in vitro* than *in vivo* (*P*<0.01). The digital flexor muscles originate on the medial epicondyle of the humerus; thus, the locking of the elbow joint in the *in vitro* loading system removed any extensor effect of the digital flexor muscles at the elbow joint. It is likely that the difference between the *in vitro* and *in vivo* stiffness observed here is due, in part, to the removal of the link that the elbow joint provides between the distal and proximal springs *in vivo*. The elbow gradually extends through stance (Back et al., 1995), which will allow the digital flexor muscle bellies to shorten. Much of the load is transmitted through the accessory ligaments that bypass the muscle and attach within the distal limb, so this effect will be limited. An additional contributing factor to the differences between the *in vitro* and *in vivo* plots is the orientation of the limb during *in vitro* loading. *In vivo* at trot the limb sweeps through an angle of approximately 27° during the loading phase of stance and a similar angle during the unloading phase, whereas *in vitro* the limb was orientated vertically during loading and unloading. A previous study has shown that the orientation of the limb through the stance phase has a small effect on limb stiffness (Wilson et al., 2001b).

Comparison of Figs 5 and 9 demonstrates that on the soft surface, limb loading and MCP joint angle rise more slowly than on the hard surface. The surface acts as a visco-elastic element in series with the proximal and distal limb springs (Gerritsen et al., 1995). A compliant surface therefore reduces the stiffness the spring mass system as a whole, reducing its resonant frequency and, hence, rate of force rise (Wilson et al., 2001b). The unloading curves are, however, similar on both surfaces. This is because equestrian surfaces undergo plastic rather than elastic deformation (Zebarth and Sheard, 1985), which appears, mechanically, as a reduced stiffness on loading (i.e. a greater shortening of the spring system for the rise in GRF from zero at foot-on to peak force), but because the surface does not 'return' there is no concomitant effect during unloading. The relationship between GRF and MCP joint angle does not appear to change as a function of surface, which is further evidence for little or no capacity to tune the distal spring. If a horse tuned its limb for the surface, as seen in man (Ferris and Farley, 1997), then perhaps the limb would be less compliant during loading on the soft surface but have the same compliance during unloading on both surfaces, i.e. the hysteresis loop of MCP angle against vertical GRF would change as a function of surface plasticity. This is not evident in our data. The viscous nature of the soft surface also accounts for the more rapid damping of the high frequency vibrations in the GRF curve on the soft surface (Wilson et al., 2001b). The more gradual rise in GRF should also result in an increase in stance time/duty factor, explaining why horses gallop more slowly on soft ground.

The *in vivo* MCP joint angle–vertical GRF relationship was not identical on limb loading and unloading. There are two possible explanations for this: (1) approximately 7% of elastic strain energy is dissipated as heat within the tendon rather than returned (Ker et al., 1981; Riemersma and Schamhardt, 1985; Wilson and Goodship, 1994); (2) the DIP joint and elbow joint extend through stance. This transfers load to the deep digital flexor tendon *via* the accessory ligament and allows the deep digital flexor muscle to shorten (since the origin of the muscles moves distally as the elbow extends). The accessory ligament is shorter and stiffer than the muscle belly, so an increase in muscle-tendon unit and hence limb stiffness will occur.

The linear relationship between MCP joint angle and limb force would be expected, since tendon is linearly elastic once loaded beyond its toe region (Riemersma and Schamhardt, 1985) and the moment arm of the tendons on the MCP joint is relatively independent of joint angle. The MCP joint angle can therefore be used to predict limb force from kinematic data either by pre-calibration of the horse of interest using a forceplate during low speed gait or, given the similarity between horses, from the population average reported here. Direct measurement of the GRF at gallop is difficult because stride length at gallop (approximately 6 m; Rooney, 1986) is much longer than standard forceplates resulting in a probability of about one in ten that any one foot will strike the forceplate. Due to the physiological and mechanical stress that high-speed gallop places on the horse it is very difficult to achieve a sufficient number of forceplate strikes to provide meaningful data. Force measuring shoes have been used (Barrey, 1990; Kai et al., 1999; Ratzlaff et al., 1997), but the data is often difficult to relate to the GRF; also they are difficult to build for reliable measurement on soft surfaces and their mass can interfere with normal gait, as the horse's foot accelerates at approximately 400 m s^{-2} at foot-off (A. M. Wilson, unpublished data). The peak limb forces predicted here from joint angle data for the non-lead forelimb (13.51–17.10 N kg^{-1} BM) are similar to the limited data (one horse) published elsewhere using direct measurement with a forceplate, which states a peak vertical GRF of 1.7× body mass (Kingsbury et al., 1978).

Conclusion

The hypothesis that most of the length change during stance in the equine limb occurs in the distal segment was proven. There is no evidence from this study that distal limb compliance changes in response to gait or muscle activation, supporting the second hypothesis. There may, however, be limited scope for tuning limb compliance *via* changing activation of the muscles of the proximal segment. The linear relationship between MCP joint angle and limb force may be used to predict limb force from kinematic data.

References

Alexander, R. McN. (1988). *Elastic Mechanisms in Animal Movement*. Cambridge University Press, Cambridge.

Alexander, R. McN. and Bennet-Clarke, H. C. (1977). Storage of elastic strain energy in muscles and other tissues. *Nature* **265**, 114-117.

Alexander, R. McN., Maloiy, G. M. O., Ker, R. F., Jayes, A. S. and Warui, C. N. (1982). The role of tendon elasticity in the locomotion of the camel (*Camelus dromedarius*). *J. Zool. Lond.* **198**, 293-313.

Alexander, R. McN., Maloiy, G. M. O., Njau, R. and Jayes, A. S. (1979). Mechanics of running of the ostrich (*Struthio camelus*). *J. Zool. Lond.* **187**, 169-178.

Back, W., Schamhardt, H. C., Savelberg, H. H. C. M., Bogert, A. J. van den, Bruin, G., Hartman, W. and Barneveld, A. (1995). How the horse moves: 1. Significance of graphical representations of equine forelimb kinematics. *Equine Vet. J.* **27**, 31-38.

Barrey, E. (1990). Investigation of the vertical hoof force distribution in the equine forelimb with an instrumented horseboot. *Equine Vet. J.* **Suppl. 9**, 35-38.

Biewener, A. A. (1983). Allometry of quadrupedal locomotion: the scaling of duty factor, bone curvature and limb orientation to body size. *J. Exp. Biol.* **105**, 147-171.

Biewener, A. A. (1998a). Muscle-tendon stresses and elastic energy storage during locomotion in the horse. *Comp. Biochem. Physiol. B* **120**, 73-87.

Biewener, A. A. (1998b). Muscle function *in vivo*: a comparison of muscles used for elastic energy savings *versus* muscles used to generate mechanical power. *Amer. Zool.* **38**, 703-717.

Biewener, A. A., Konieczynski, D. D. and Baudinette, R. V. (1998). *In vivo* muscle force–length behaviour during steady speed hopping in tammar wallabies. *J. Exp. Biol.* **201**, 1681-1694.

Biewener, A. A. and Roberts, T. J. (2000). Muscle and tendon contribution to force, work and elastic energy savings: a comparative perspective. *Ex. Sports Sci. Rev.* **28**, 99-107.

Birch, H. L., McLaughlin, L., Smith, R. K. and Goodship, A. E. (1999). Treadmill exercise induced tendon hypertrophy: assessment of tendons with different mechanical functions. *Equine Vet. J.* **Suppl. 30**, 222-226.

Blickhan, R. (1989). The spring-mass model for running and hopping. *J. Biomech.* **22**, 1217-1227.

Bogert, A. J., Gerritsen, K. G. M. and Cole, G. K. (1988). Human muscle modeling from a user's perspective. *J. Electromyog. Kinesiol.* **8**, 119-124.

Buchner, H. H. F., Savelberg, H. H. C. M., Schamhardt, H. C., Merkens, H. W. and Barneveld, A. (1994). Habituation of horses to treadmill locomotion. *Equine Vet. J.* **Suppl. 17**, 13-15.

Cavagna, G. A., Heglund, N. C. and Taylor, C. R. (1977). Mechanical work in terrestrial locomotion: two basic mechanisms for minimizing energy expenditure. *Am. J. Physiol.* **233**, R243-R261.

Clayton, H. M., Lanovaz, J. L., Schamhardt, H. C. and van Wessum, R. (1999). The effect of rider's mass on ground reaction forces and fetlock kinematics at the trot. *Equine Vet. J.* **Suppl. 30**, 218-221.

Dimery, N. J., Alexander, R. McN. and Ker, R. F. (1986). Elastic extension of leg tendons in the locomotion of horses (*Equus caballus*). *J. Zool. Lond.* **210**, 415-425.

Dyce, K. M., Sack, W. O. and Wensing, C. J. G. (ed.) (1987). *Textbook of Veterinary Anatomy* 2nd Edition. London, Saunders.

Farley, C. T., Blickhan, R., Satio, J. and Taylor, C. R. (1991). Hopping frequency in humans: a test of how springs set stride frequency in bouncing gaits. *J. Appl. Physiol.* **71**, 2127-2132.

Farley, C. T., Glasheen, J. and McMahon, T. A. (1993). Running springs: speed and animal size. *J. Exp. Biol.* **185**, 71-86.

Farley, C. T. and Gonzales, O. (1996). Leg stiffness and stride frequency in human running. *J. Biomech.* **29**, 181-186.

Farley, C. T., Houdijk, H. H. P., Strien, C. van and Louie, M. (1998). Mechanism of leg stiffness adjustment for hopping on surfaces of different stiffnesses. *J. Appl. Physiol.* **85**, 1044-1055.

Ferris, D. P. and Farley, C. T. (1997). Interaction of leg stiffness and surface stiffness during human hopping. *J. Appl. Physiol.* **82**, 15-22.

Gerritsen, K. G. M., van den Bogert, A. J. and Nigg, B. M. (1995). Direct dynamics simulation of the impact phase in heel-toe running. *J. Biomech.* **28**, 661-668.

Hermanson, J. W. and Cobb, M. A. (1992). Four forearm flexor muscles of the horse, *Equus caballus*: anatomy and histochemistry. *J. Morph.* **212**, 269-280.

Kai, M., Takahashi, T., Aoki, O. and Oki, H. (1999). Influence of rough track surfaces on components of vertical forces in cantering thoroughbred horses. *Equine Vet. J.* **Suppl. 30**, 214-217.

Ker, R. F. (1981). Dynamic tensile properties of the plantaris tendon of sheep (*Ovis aries*). *J. Exp. Biol.* **93**, 283-302.

Kingsbury, H. B., Quddus, M. A., Rooney, J. R. and Geary, J. E. (1978). A laboratory system for production of flexion rates and forces in the forelimb of the horse. *Am. J. Vet. Res.* **39**, 365-369.

Leach, D. and Cymbaluk, N. F. (1986). Relationship between stride length, stride frequency, velocity and morphometrics in foals. *Am. J. Vet. Res.* **47**, 2090-2097.

McLaughlin, D. M., Gaughan, E. M., Roush, J. K. and Skaggs, C. L. (1996). Effects of subject velocity on ground reaction force measurements and stance times in clinically normal horses at walk and trot. *Am. J. Vet. Res.* **57**, 7-11.

McMahon, T. A. (1985). The role of compliance in mammalian running gaits. *J. Exp. Biol.* **115**, 263-282.

McMahon, T. A. and Cheng, G. C. (1990). The mechanics of running: how does stiffness couple with speed? *J. Biomech.* **23 Suppl.** 1, 65-78.

McMahon, T. A. and Greene, P. R. (1979). The influence of track compliance on running. *J. Biomech.* **12**, 893-904.

Meershoek, L. S., Schamhardt, H. C., Roepstorff, L. and Johnston, C. (2001). Forelimb tendon loading during jump landings and the influence of fence height. *Equine Vet. J.* **Suppl. 33**, 6-10.

Merkens, H. W., Schamhardt, H. C., Hartman, W. and Kersjes, A. W. (1985). Ground reaction force patterns of Dutch Warmblood horses at normal walk. *Equine Vet. J.* **18**, 207-214.

Minetti, A. E., Ardigo, L. P., Reinach, E. and Saibene, F. (1999). The relationship between mechanical work and energy expenditure of locomotion in horses. *J. Exp. Biol.* **202**, 2329-2338.

Pratt, G. W. and O'Connor, J. T. (1978). A relationship between gait and breakdown in the horse. *Am. J. Vet. Res.* **39**, 249-253.

Ratzlaff, M. H., Hyde, M. L., Hutton, D. V., Rathgeber, R. A. and Balch, O. K. (1997). Interrelationships between moisture content of the track, dynamic properties of the track and the locomotor forces exerted by galloping horses. *Equine Vet. Sci.* **17**, 35-42.

Riemersma, D. J. and Schamhardt, H. C. (1985). In vitro mechanical properties if equine tendons in relation to cross sectional area and collagen content. *Res. Vet. Sci.* **39**, 263-270.

Roberts, T. J., Marsh, R. L., Weyand, P. G. and Taylor, C. R. (1997). Muscular force in running turkeys: the economy of minimising work. *Science* **275**, 1113-1115.

Rooney, J. R. (1986). A model for horse movement. *J. Equine Vet. Sci.* **6**, 30-34.

Rubin, C. T. and Lanyon, L. E. (1987). Kappa Delta Award paper: Osteoregulatory nature of mechanical stimuli: function as a determinant of adaptive bone remodelling. *J. Orthop. Res.* **5**, 300-310.

Stephens, P. R., Nunamaker, D. M. and Butterweck, D. M. (1989). Application of a Hall-effect transducer for measurement of tendon strains in horses. *Am. J. Vet. Res.* **50**, 1089-1095.

van Weeren, P. R., van den Bogert, A. J. and Barneveld, A. (1990). A quantitative analysis of skin displacement in the trotting horse. *Equine Vet. J.* **Suppl. 9**, 101-109.

Williams, R. B., Harkins, L. S., Hammond, C. J. and Wood, J. L. N. (2001). Racehorse injuries, clinical problems and fatalities recorded on British racecourses from flat racing and National Hunt racing during 1996, 1997 and 1998. *Equine Vet. J.* **33**, 478-486.

Wilson A. M. (1991). The effect of exercise intensity on the biochemistry, morphology and biochemistry of tendon. PhD thesis University of Bristol.

Wilson, A. M., van den Bogert, A. J. and McGuigan, M. P. (2000). Optimization of the muscle-tendon unit for economical locomotion in cursorial animals. In *Skeletal Muscle Mechanics: From Mechanism to Function* (ed. W. Herzog), pp. 517-547. Chichester, England: John Wiley and Sons Ltd.

Wilson, A. M., McGuigan, M. P., Fouracre, L. and MacMahon, L. (2001a). The force and contact stress on the navicular bone during trot locomotion in sound horses and horses with navicular disease. *Equine Vet. J.* **32**, 159-165.

Wilson, A. M. and McGuigan, M. P., Su, A. and van den Bogert, A. J. (2001b). Horses damp the spring in their step. *Nature* **414**, 895-899.

Wilson, A. M., Watson, J. C. and Lichtwark, G. A. (2003). A catapult action for rapid limb protraction *Nature* **421**, 35-36.

Wilson, A. M. and Goodship, A. E. (1994). Exercise-induced hyperthermia as a possible mechanism for tendon degeneration. *J. Biomech.* **27**, 899-905.

Wilson, A. M., Seelig, T. J., Shield, R. A. and Silverman, B. W. (1998). The effect of hoof inbalance on point of force application in the horse. *Equine Vet. J.* **30**, 540-545.

Zebarth, B. J. and Sheard, R. W. (1985). Impact and shear resistance of turf and grass racing surfaces for Thoroughbreds. *Am. J. Vet. Res.* **46**, 778-784.